

Application of Artificial Neural Networks to the prediction of out-of-plane response of infill walls subjected to shake table

Onur Onat*¹ and Muhammet Gul^{2a}

¹Department of Civil Engineering, Munzur University, Aktuluk Campus, 62000, Tunceli, Turkey

²Department of Industrial Engineering, Munzur University, Aktuluk Campus, 62000, Tunceli, Turkey

(Received August 15, 2017, Revised March 6, 2018, Accepted March 8, 2018)

Abstract. The main purpose of this paper is to predict missing absolute out-of-plane displacements and failure limits of infill walls by artificial neural network (ANN) models. For this purpose, two shake table experiments are performed. These experiments are conducted on a 1:1 scale one-bay one-story reinforced concrete frame (RCF) with an infill wall. One of the experimental models is composed of unreinforced brick model (URB) enclosures with an RCF and other is composed of an infill wall with bed joint reinforcement (BJR) enclosures with an RCF. An artificial earthquake load is applied with four acceleration levels to the URB model and with five acceleration levels to the BJR model. After a certain acceleration level, the accelerometers are detached from the wall to prevent damage to them. The removal of these instruments results in missing data. The missing absolute maximum out-of-plane displacements are predicted with ANN models. Failure of the infill wall in the out-of-plane direction is also predicted at the 0.79 g acceleration level. An accuracy of 99% is obtained for the available data. In addition, a benchmark analysis with multiple regression is performed. This study validates that the ANN-based procedure estimates missing experimental data more accurately than multiple regression models.

Keywords: artificial neural network; out-of-plane response; infill wall; earthquake; reinforced concrete frame

1. Introduction

Shake table experiments are the most suitable methods for determining the response of structural elements under real or artificial earthquake motion. These types of experiments are more reliable due to complete simulation of the structures. Basically, a shake table is composed of a platform on hydraulic pillars that enables a scaled structure to be shaken. To shake the platform, hydraulic actuators are used. However, shake table experiments are more expensive than quasi-static, cyclic-monotonic, and pseudo-dynamic tests (Mendes 2012). Experimental prediction of the in-plane and out-of-plane responses of the infill wall is necessary to prevent its failure during ground excitation, because out-of-plane failure of the infill wall may result in loss of both life and property. Out-of-plane failure occurs due to the combined behavior of the infill wall in the in-plane and out-of-plane directions. Many researchers investigated the in-plane behavior of the infill wall and proposed equations to estimate its capacity (Dolsek and Fajfar 2002, Shing and Mehrabi 2002, Al-Chaar *et al.* 2002, Anil and Altın 2007, Pereira 2013). Experience with earthquakes all over the world shows that out-of-plane failure of infill walls is the major reason for both loss of life and economic losses. This fact motivated researchers to

perform theoretical and experimental studies on infill walls to investigate global and local behavior (Onat *et al.* 2015, Onat *et al.* 2016, Lourenço *et al.* 2016, Yön *et al.* 2017). D'Ayala and Shi (2011) performed shake table tests on three dry masonry specimens 1/10 scaled to investigate the behavior of historical masonry structures by using multi-rigid body dynamics (D'Ayala and Shi 2011, Shi 2016). The seismic behavior of masonry walls with an out-of-plane-direction earthquake load was investigated by Al Shawa *et al.* (2012). The dynamic responses of single and cavity masonry walls with different tie orientations were investigated by Graziotti *et al.* (2016). The out-of-plane response under bidirectional earthquake loads was investigated by Calvi and Bolognini (2001), Hashemi and Mosalam (2006), Pujol and Fick (2010), Varela-Rivera *et al.* (2011), Stavridis *et al.* (2012), Misir *et al.* (2012), Varela-Rivera *et al.* (2012), and Vaculik and Griffith (2017). In-plane and out-of-plane interactions of the infill wall during earthquakes directly affect first the structural rigidity and then the progressive collapse mechanism (Mosalam and Gunay 2015). Comparing the quantitative study with the experimental study is a common method that employs a software to classify out-of-plane damage according to the infill drift level via displacement, as indicated by Tu *et al.* (2010). During the out-of-plane tests, it is important to estimate the snapped through displacement of the infill wall. However, after a large horizontal displacement, the accelerometers, LVDTs, or potentiometers are removed to protect the devices from further damage during the early phase of the test, as emphasized by Valera-Rivera (2016). Furtado *et al.* (2016) implemented a series of tests on the infill masonry wall to determine the effect of in-plane

*Corresponding author, Assistant Professor,
E-mail: onuronat@munzur.edu.tr

^a Ph.D.

E-mail: muhammetgul@munzur.edu.tr

damage on out-of-plane failure of the infill wall. For this purpose, a full-scale double-leaf infill wall panel was tested. However, to prevent out-of-plane total collapse of the infill wall and data loss, in-plane damage was kept at the 0.5% drift level, and additional apparatus were used in the test. Misir et al. (Misir *et al.* 2015, 2016) applied 30% of the in-plane load in the out-of-plane direction of the tested specimen to assess the performance of infill walls under a bidirectional load. The reason for applying a proportional load in the out-of-plane direction is the sensitivity and slenderness due to in-plane damage. During a series of experimental tests implemented by Shan *et al.* (2016), a few instruments were disabled before the end of the test. Disabling the instruments causes missing data, which prevents correct evaluation of the data after the experimental tests.

Experimental assessment of the out-of-plane capacity or the out-of-plane response of the infill wall under an earthquake load is difficult due to the slenderness of the infill wall in the out-of-plane direction. Each test suffers from missing data due to early removal of instruments. In this study, a new concept is developed to prevent missing data by employing ANN-based prediction. To this end, two shake table experiments were selected as an unreinforced brick model (URB) and a bed joint reinforcement (BJR) model. The BJR model is selected as the benchmark model for prediction. A high level of accuracy is obtained for missing data prediction. In addition to missing data prediction, absolute maximum displacements are predicted for both models at the 0.79 g PGA level to plot the out-of-plane failure mode of the infill wall at the time of its total collapse.

The rest of the paper is structured as follows: The next section presents related reviews of the literature and reveals the research gap that this paper addresses. Section 3 provides experimental data. Section 4 offers a general overview of ANNs and the proposed methodology. Section 5 presents the results and discusses of the application study. Finally, Section 6 presents the conclusions, limitations, and recommendations for future studies.

2. Literature review of ANN studies

Forecasting of events is a topic that comes under civil engineering applications. Recently, artificial neural networks (ANNs) have emerged as an attractive forecasting technique applicable to a vast number of civil engineering problems including structural mechanics (Sakla and Ashour 2005, Kişi and Cigizoglu 2007, Bilgehan *et al.* 2012, Kumar and Samui 2013, Sipos *et al.* 2013, Garzon-Roca *et al.* 2013, Lanza di Scalea 2006, Fahmy *et al.* 2016), structural material science (Topçu *et al.* 2009, Hoła and Schabowicz 2005, Joshi *et al.* 2014), and others (Hasańcebi and Dumlupınar 2013, Hakim and Razak 2014). An important characteristic of modeling with ANNs is the ability to estimate missing values without having to measure them. In particular, such infill wall models can be constructed after a training process with available data, which can be used to predict the absolute out-of-plane

displacement parameter, saving time and money when performing experiments.

The literature includes studies in which ANNs are used in structural mechanics problems for prediction. Sipos *et al.* (2013) applied ANNs to predict the seismic behavior of framed masonry buildings. Because the study was motivated by a higher uncertainty and many parameters were included in the estimation of their seismic capacity, a multilayer back propagation neural network with an adaptive weighting function algorithm was used for the applied neural network architecture. In another study, Garzon-Roca *et al.* (2013) proposed a model to estimate the load-bearing capacity of brick masonry walls. Apart from carrying out various analytical, experimental, and numerical studies on the behavior of brick masonry walls that originate from specific theories and vary in precision and complexity, a novel ANN-based formulation was proposed to estimate the axial behavior of brick masonry walls. Both for the above-mentioned two studies and for the study we proposed, models are composed of a large number of interconnected processing elements tied together with weighted connections that work in parallel to solve the problems of interest. ANNs are mostly suitable for situations where classical constitutive modeling may be insufficient and time consuming. One of their most important characteristic is that they can learn even in the case of incomplete data, and make reliable predictions on datasets that are new to them (Hasańcebi and Dumlupınar 2013). Eventually, their unique learning and prediction characteristics led to their application to problems encountered in various civil engineering applications.

Table 1 shows a comparative summary of previous studies on the usage of ANNs in the civil engineering context in terms of objectives, approach followed, performance measures, and accuracy of results.

From the overview of the above-mentioned previous works, it is concluded that use of ANN models in predicting the absolute maximum out-of-plane displacement response of the infill wall and reinforced concrete frame (RCF) subjected to shake table excitation as a special subject of civil engineering is indeed novel and appropriate. Shake table experiments are very expensive, but they are one of the best methods to simulate the actual behavior of structural response. However, during these test procedures, the main challenge is to determine the response limits of the structure under strong excitation. This is because, during the process of determining the structural response, most of the tested models sustain heavy damage or collapse, necessitating disposal of measurement devices. Damage to instruments can be expensive and can result in missing data. To lower to cost of shake table experiments, prediction of data prediction of data after removal of devices from the tested specimen could be a viable option. To the best of the authors' knowledge, no work has been reported in the literature that applies ANNs for estimation of the out-of-plane response of infill walls subjected to shake table excitation. This is the main motivation for this study.

Table 1 Comparison of the previous studies that have used ANNs in civil engineering context

Study	Objectives	Approach used	Performance measures and results
Topçu <i>et al.</i> (2009)	To model corrosion currents of reinforced concrete	A feed forward ANN with 4 inputs (Fly Ash Ratio, Cement Type, Curing Time, Time Interval) and 1 output (Corrosion Current) is proposed.	As performance measure, mean absolute percentage error-MAPE (9.4371), root mean squared error-RMSE (0.0114) and Correlation coefficient (0.9941) were used. On conclusion of the study, accurate prediction results for corrosion currents were obtained using ANN.
Lee and Han (2002)	Developing an ANN model for the generation of artificial earthquake and response spectra	5 ANN models for replacing traditional processes are constructed.	The study shows that procedure using ANN models is applicable to generate artificial earthquakes and response spectra.
Sakla and Ashour (2005)	Developing an ANN model to predict the tensile capacity of single adhesive anchors	A back-propagation ANN with Levenberg–Marquardt training algorithm and Bayesian regularization is proposed using 7 design variables as inputs and the uniform bond strength of adhesive anchors as the output.	The results show that the MAPE is 16.8% and 14.1% and the coefficient of correlation, R2, is 0.935 and 0.941 for the training and testing data sets, respectively.
Kişi and Cigizoglu (2007)	Presenting various ANN models for short- and long-term continuous and intermittent daily streamflow forecasting	3 different ANN methods as feed-forward back propagation, generalized regression neural networks, and radial basis function-based ANNs are applied to continuous and intermittent river flow data of 2 Turkish rivers.	The study concludes that the forecasting performance of radial basis function based ANN is found to be superior to the other two ANN methods.
Hola and Schabowicz (2005)	Developing an ANN model to determine strength of concrete on the basis of non-destructively determined tests	5 different multilayer error back-propagation ANNs (Levenberg–Marquardt, conjugate gradient, descent gradient, and etc.) are used for the task.	The results show that the ANN models are highly suitable for assessing the compressive strength of concrete.
Bilgehan <i>et al.</i> (2012)	Proposing an ANN based model for buckling analysis of slender prismatic columns with a single non-propagating open edge crack subjected to axial loads	A multilayer feedforward ANN learning by backpropagation algorithm is proposed. 4 critical buckling load estimation models are run in terms of support condition of columns and rods under compression.	The results show that the model with fixed-fixed support condition has the smallest RMSE (0.13) and the highest R2 (0.996)
Kumar and Samui (2013)	Using of ANN for predicting pore water pressure response in a shake table test	A multilayer feed-forward back-propagation network, which was created by generalizing the Levenberg-Marquardt algorithm is constructed.	The results of the study indicate that the linear coefficient of correlation is very high between observed experimental data and values predicted through ANNs and it is 0.972 for training data and 0.956 for test data.
Sipos <i>et al.</i> (2013)	Revealing earthquake performance of infilled frames using ANNs	A multilayered back propagation ANN with adaptive weight function is applied and the optimal network topology.	The study concludes that the best predictions of the output values had neural network with 4 neurons in one hidden layer (for failure mode MSE=1.214 and R=0.874).
Garzon-Roca <i>et al.</i> (2013)	Estimation of the axial behaviour of masonry walls based on ANNs	An ANN based proposal is presented considering load eccentricity, wall slenderness ratio and stiffness and masonry tensile strength.	The experimental results and is less conservative than Eurocode 6 and therefore more likely to provide the optimum design for masonry walls.
Hasançebi and Dumlupınar (2013)	Developing an ANN model for finite element model updating of reinforced concrete T-beam bridges	Levenberg-Marquardt back-propagation algorithm is proposed for model updating procedure for the RC T-beam bridge.	The results show that n average order of errors can be effectively reduced to 2.91% for dynamic responses and to 5.40% for static responses using ANN.
Facchini <i>et al.</i> (2014)	Proposing the application of ANNs for output-only modal identification of structural systems	A feed-forward back-propagation ANN is adopted for the recognition of the structural eigenvalues and eigenmodes.	The proposed model is tested on a three-storey steel-frame and the results show that it can be able to assess eigenvalues and eigenmodes, as demonstrated by comparison of the obtained results with those provided by literature methods.
Joshi <i>et al.</i> (2014)	Application of ANNs for dynamic analysis of building frames	ANN models in 3 categories varying the number of input parameters which are mass, stiffness and geometry of the buildings for each one is proposed.	The results show that the values obtained through the ANN models are close to the experimental values
Fahmy <i>et al.</i> (2016)	Developing an ANN model for conceptual design of orthotropic steel-deck bridge	The development of preliminary design system for orthotropic bridge steel decks using the concept of ANN is proposed.	The results show that the ANN model for the selection of orthotropic deck dimensions is a better and cost-effective option compared with international codes or expert opinion.

3. Experimental data

Experimental data for this study are obtained from two shake table experiments carried out in a laboratory in Portugal (Onat 2015). In this study, the purpose of the shake table experiment series is to assess the local out-of-plane behavior of an infill wall enclosed by an RCF. For this purpose, a one-bay and one-story 1:1 scale RCF and infill wall are constructed. The full test setup and one of the tested specimens are shown in Fig. 1.

Two specimens that will be subjected to shake table excitation are constructed. One of the specimens consists of an unreinforced brick infill wall, and the other is an infill wall reinforced with BJR. In-plane and out-of-plane ground motion are applied bidirectionally and simultaneously to each tested specimen. The out-of-plane response is recorded with 12 accelerometers from the infill wall and 8 accelerometers from the RCF. Absolute maximum displacements are obtained from the derived accelerations (Onat 2015). A schematic view of the tested specimens is shown in Fig. 2.



Fig. 1 Full test set up and tested specimen (Onat 2015, Correira *et al.* 2014)

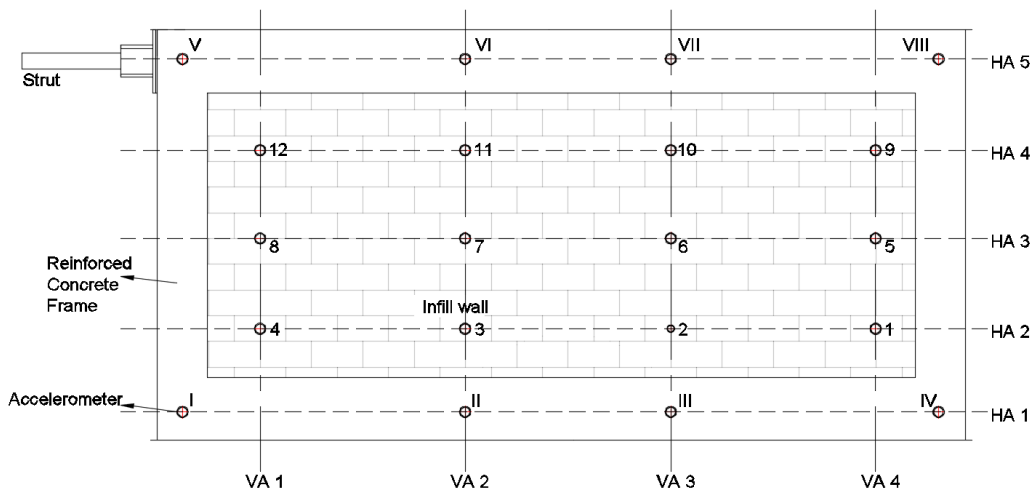


Fig. 2 Vertical and horizontal alignment number of accelerometers on tested infill wall

There are four vertical alignments and five horizontal alignments on the test specimens as seen in Fig. 2. The purpose of these alignments is to give a coordinate to each accelerometer and to plot the out-of-plane displacement in order to observe the failure mode of the infill wall. There is also a supplementary equipment called STRUT. The mission of STRUT in these shake table experiments is to keep the test specimens stable along the in-plane direction. The term *in-plane direction* refers to the longitudinal direction of the test specimens, and the term *out-of-plane direction* refers to the direction perpendicular to the planar surface of the infill wall. These experiments were carried out with an artificially produced earthquake time series according to their return period as indicated in Eurocode-8. These earthquake data are presented in Table 2.

Table 2 Seismic input intensities at each stage for both URB and BJR models

Stage	PGA (g)	
	URB	BJR
1	0.04	0.05
2	0.18	0.15
3	0.29	0.38
4	0.53	0.74
5	0.79	*

* Stage 5 shake table experiment has not performed for BJR model

Table 3 Descriptions of input and output variables

Parameters	Unit	Variable type	Detail	
			Model-I (URB)	Model-II (BJR)
PGA	g	Input	Each data set consists of four PGA values as 0.04, 0.18, 0.28, 0.53	Each data set consists of five PGA values as 0.05, 0.15, 0.38, 0.59, 0.74
Local weight	tonne	Input	(i) First data set consists of four local weight values as 0.1, 0.142, 0.15, 0.23 (ii) Second data set consists of two local weight values as 0.641, 0.738	
Vertical distance from strut	m	Input	(i) First data set consists of five vertical distance values as 1.1, 1.11, 1.64, 2.15, 2.16 (ii) Second data set consists of two vertical distance values as 0.2, 3.0	
Horizontal distance from strut	m	Input	(i) First data set consists of four horizontal distance values as 0.6, 2.46, 3.95, 5.8 (ii) Second data set consists of four horizontal distance values as 0.2, 2.46, 3.95, 6.2	
Absolute maximum out-of-plane displacement	mm	Output	(i) For first data set [min, max, mean, SD]= [1.08, 16.60, 6.99, 4.54] (ii) For second data set [min, max, mean, SD]= [1.05, 18.10, 6.79, 4.66]	(i) For first data set [min, max, mean, SD]= [0.78, 73.90, 10.36, 14.87] (ii) For second data set [min, max, mean, SD]= [0.8, 55.8, 10.5, 11.3]

min, max, mean, SD denote minimum, maximum, the mean and standard deviation, respectively

Table 4 Absolute maximum displacement (mm) of BJR model for 0.59 g ground motion level and missing data

Absolute maximum displacement (mm)		Vertical alignment of accelerometer position			
Horizontal alignment of accelerometer position		VA1	VA2	VA3	VA4
	HA5	13.7	13.1	20.0	12.4
	HA4	38.6	*	23.2	*
	HA3	14.4	*	*	14.3
	HA2	*	*	33.0	14.6
	HA1	13.5	12.9	12.7	13.1

*Missing data due to removing instruments on the wall

Table 5 Absolute maximum displacement (mm) of BJR model for 0.74 g ground motion level and missing data

Absolute maximum displacement (mm)		Vertical alignment of accelerometer position			
Horizontal alignment of accelerometer position		VA1	VA2	VA3	VA4
	HA5	55.82	*	40.6	*
	HA4	*	*	51.7	*
	HA3	73.9	*	*	*
	HA2	*	*	40	*
	HA1	21.4	*	20.8	*

*Missing data due to removing instruments on the wall

Data used in both models (URB and BJR models) of the study consist of two different sets. Whereas the first data set pertains to the infill wall, the second data set deals with the RCF. Each data set has four input parameters (peak ground acceleration-PGA, local weight, vertical distance from STRUT, and horizontal distance from STRUT) and one output parameter (absolute maximum out-of-plane displacement). The statistical results for the predictor types

are presented in Table 3. Once the ANN model is constructed, the input parameters are divided into four groups: the PGA of the shake table, the local weight, and horizontal and vertical distances from STRUT. The local weight is one of the most important parameters that affects the recorded absolute maximum displacement because each accelerometer controls a different amount of weight. The horizontal and vertical distances from STRUT keep the

magnitude of displacement very high due to the operating mechanism. The STRUT mechanism keeps the infill wall stable in the in-plane direction. Moreover, there are two hinges located at the end points of STRUT. These hinges allow the tested specimens to move freely in the out-of-plane direction. For this reason, there is a direct correlation between the location of the accelerometers and STRUT on the RCF and infill wall.

Shake table experiments were implemented in four steps for the URB model and in five steps for the BJR model. The PGA values of each test step can be seen in Table 3. During the first test, which is carried on the URB model, shake table experiments could not continue for 0.79 g due to local failure of the infill wall and total collapse risk of the complete infill wall in the out-of-plane direction. The shake table experiments at 0.79g were implemented on the BJR model, but much data could not be captured due to heavy cracks in the infill wall. When crack propagation began, the accelerometers on the wall were removed in order not to damage the instruments. For this reason, the out-of-plane response could not be measured in some places for Model-II. These missing data can be seen in Table 4 for the 0.59 g ground motion level and in Table 5 for the 0.74 g ground motion level.

All displacements were obtained from the accelerometer. This calculation was performed by double integration as seen in Eqs. (1)- (3)

$$\text{Peak Ground Acceleration (PGA)} = \max|\ddot{u}_g(t)| \quad (1)$$

$$\text{Peak Ground Velocity (PGV)} = \max|\dot{u}_g(t)| \quad (2)$$

$$\text{Peak Ground Displacement (PGD)} = \max|u_g(t)| \quad (3)$$

where $u_g(t)$ is the ground displacement as a function of time.

After calculating displacements for the test duration, absolute maximum displacements were obtained among all displacement values for the test duration.

4. Methodology

4.1 General overview of ANNs

ANNs are machine learning algorithms that work to solve computational processes in specific areas by using a large number of interconnected processing elements (Gul and Guneri 2015, 2016a, b). They are mainly used for prediction, clustering, classification, and detection of abnormal patterns (Efendigil *et al.* 2009). An ANN model, which comprises n layers, presents a different number of computational elements that function like biological neurons with numerous connections between these computational elements among layers. The computational elements used in various ANN models are called artificial neurons (Guneri and Gumus 2008, 2009). Efendigil *et al.* (2009) depicted the model flow of an artificial neuron as in Fig. 3.

In the figure, x_1, x_2, \dots, x_p are the input signals; $w_{k1}, w_{k2}, \dots, w_{kp}$ are the weights of neuron k , and u_k is the linear combiner output while θ_k denotes the threshold. Furthermore, $\Phi(\cdot)$ is the activation function; and y_k is the output of the neuron. The first layer, which is called the “input” layer, is used to obtain information from inside the network. The last layer, which is called the “output” layer, is similarly used to obtain information from outside the network. The middle layers, which are generally called “hidden” layers, are essential to the network for conversion of certain input patterns into appropriate output patterns (Somoza 1993). Information flows through the network by linear connections and linear or nonlinear transformations. The ANN’s learning can be categorized into two distinct types: supervised learning and unsupervised learning. The error between the actual output value and the predicted output value is computed. A minimization procedure is then used to adjust the weights between two connection layers, i.e., for the backpropagation model starting backward from the output layer to the input layer. There are many minimization procedures based on different optimization algorithms, such as Quasi-Newton, Levenberg–Marquardt, gradient descent, and conjugate gradient methods. In ANN models, there is a practical problem concerning the network architecture (the number of hidden layers and units in each layer) and network properties (the error and activation functions). The design of the hidden layer is dependent on the selected learning algorithm (Kröse *et al.* 1993). The more layers and neurons there are, the more complex dependencies the network can model. According to Efendigil *et al.* (2009), the number of hidden layer nodes can go up to (1) $2n + 1$ (where n is the number of nodes in the input layer), (2) 75% of the number of input parameters, or (3) 50% of the number of input and output parameters. One of the other important properties of an ANN model is the activation function for the hidden layer. The software we follow in the current research has the following functions (Alyuda 2017)

- Linear: This function produces its input as its output; in other words, it just passes the activation level directly as the output. Its output range is $[-\infty, \infty]$.
- Logistic: This function has a sigmoid curve and is calculated as follows: $F(x) = 1 / (1 + e^{-x})$. Its output range is $[0, 1]$. This function is used most often in various practical applications.
- Hyperbolic tangent: This function also has a sigmoid curve and is calculated as follows: $F(x) = (e^x - e^{-x}) / (e^x + e^{-x})$. Its output range is $[-1, 1]$. Empirically, it is often found that this function performs better than the Logistic function.

In ANNs, some controllable factors such as Learning Rate and Momentum are available to aid the learning of selected algorithms. They are control parameters used by several learning algorithms, which affect the weight changes. The higher learning rates cause higher weight changes during each iteration. The greater the momentum, the more the current weight change is affected by the weight change that took place during the previous iteration.

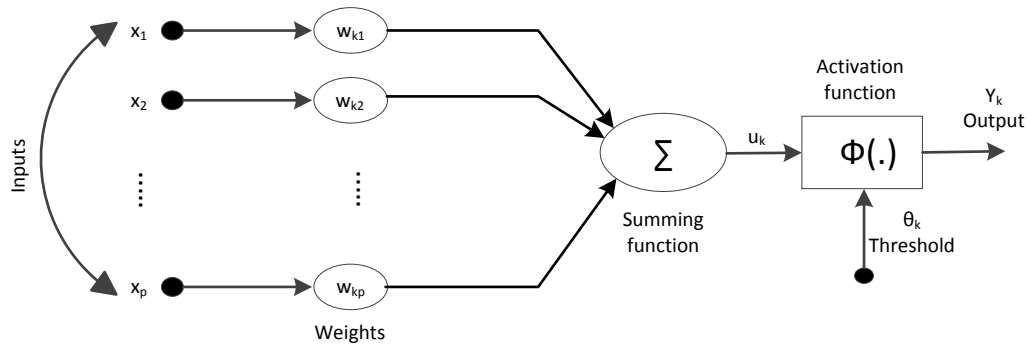


Fig. 3 Flow chart of an artificial neuron (Adapted from Efendigil *et al.* (2009))

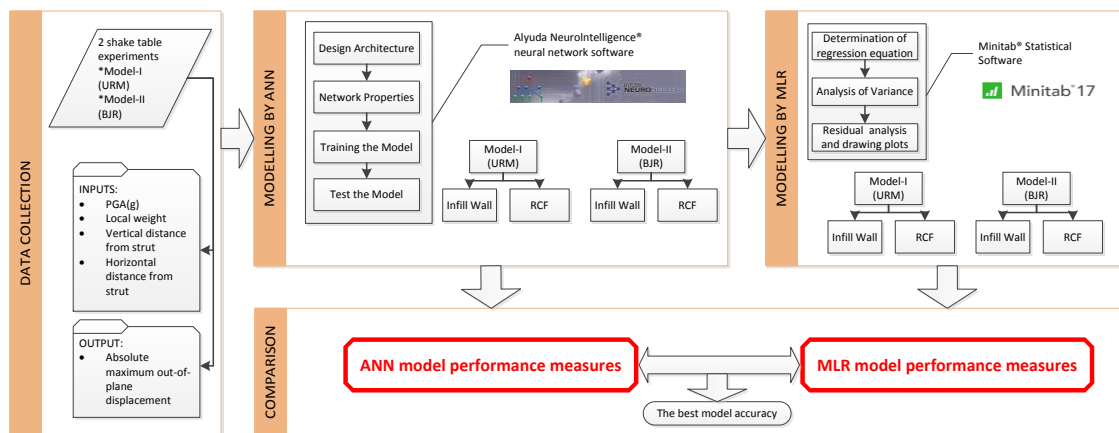


Fig. 4 A flow chart of the proposed approach

To measure the performance of ANN models, network error (average train error and average test error), absolute relative error (ARE), MSE, MAPE, and R2 can be used. MSE and MAPE are defined as in Eqs. (4) and (5)

$$MSE = \frac{1}{n} \sum_{i=1}^n (x_i - y_i)^2 \quad (4)$$

$$MAPE = \frac{100}{n} \sum_{i=1}^n \left| \frac{x_i - y_i}{x_i} \right| \quad (5)$$

4.2 The proposed ANN-based method

In this study, the main aim is to predict the missing absolute maximum out-of-plane displacement response of the infill wall and RCF. To achieve this aim, an ANN-based approach is proposed as shown in Fig. 3. First, the data of both models are combined. Model-I includes 48 and 36 data points for each of the infill wall and RCF, respectively. Similarly, Model-II has 45 and 36 data points each. This process is followed by data partition and normalization. A training and testing model based on ANN is then employed after determining the design architecture and network

properties. Finally, a comparison between the ANN model and multiple linear regression (MLR) models is carried out in order to identify which methods and models better measure the variability in the problem.

During construction of the proposed ANN model, the infill wall and RCF are predicted separately. The RCF elements are casted monolithically for a common application. However, brick infill walls are constructed one by one with mortar. The different material properties of these two elements directly affect the behavior of the complete structure. Once Model-I and Model-II are run by the ANN, the two different elements are divided into two parts like the infill wall and RCF as indicated in Fig. 4.

5. Results and discussion

5.1 Results of ANN models

An automatic selection module is used for the number of hidden layers and hidden layer neurons, iterations used during the model training, learning algorithm, and transfer functions. After the data entry, we randomly select the ratios 68:16:16 for training, validation, and testing. This means that Model-I includes 32 training, 8 validation, and 8 test data points for the infill wall and 24 training, 6 validation,

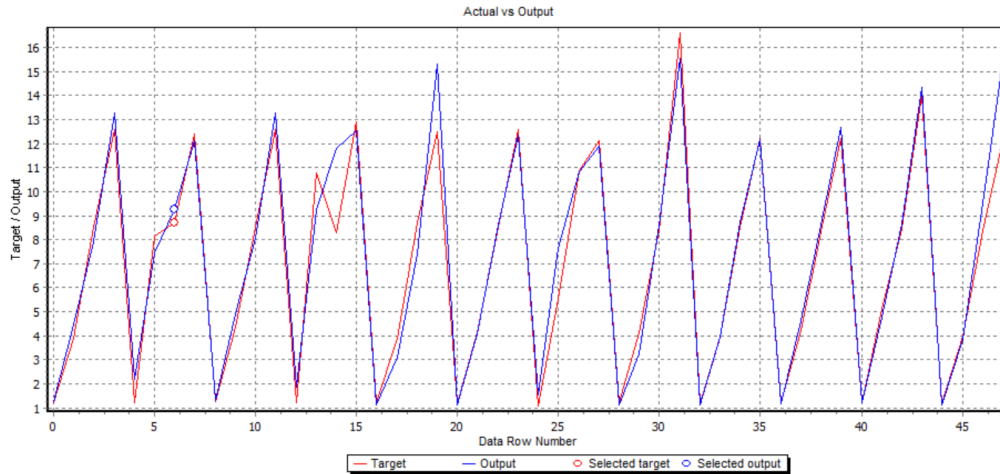


Fig. 5 Comparison of actual values and estimated output values for Model-I infill wall

Table 6 Best networks and their parameters

	Model-I (URB)		Model-II (BJR)	
	Infill wall	RCF	Infill wall	RCF
Network architecture	[4-5-1]	[4-4-1]	[4-6-1]	[4-8-1]
Training algorithm	Levenberg–Marquardt	Levenberg–Marquardt	Levenberg–Marquardt	Quasi-Newton
Hidden FX	Logistic	Logistic	Logistic	Logistic
Output FX	Logistic	Logistic	Logistic	Logistic
Number of iterations	27	43	72	1001
Average training error (mm)	0.389	0.389	0.177	1.589
Average validation error (mm)	1.325	0.5867	1.515	0.938
Average test error (mm)	0.9977	0.7099	0.259	3.618
R ²	0.98605	0.99236	0.99973	0.96618
Learning rate	0.7	0.7	0.7	0.7
Momentum	0.1	0.1	0.1	0.1

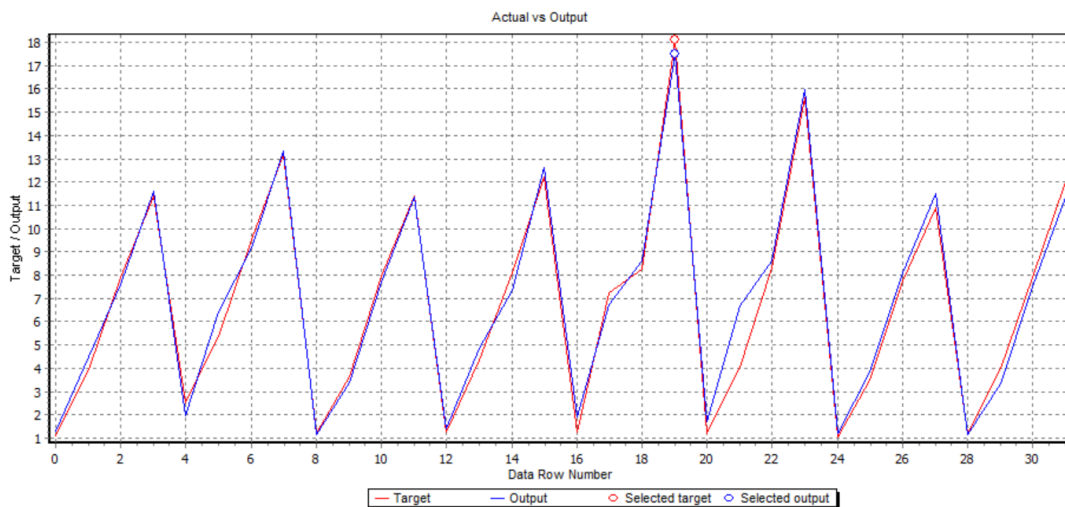


Fig. 6 Comparison of actual values and estimated output values for Model-I RCF

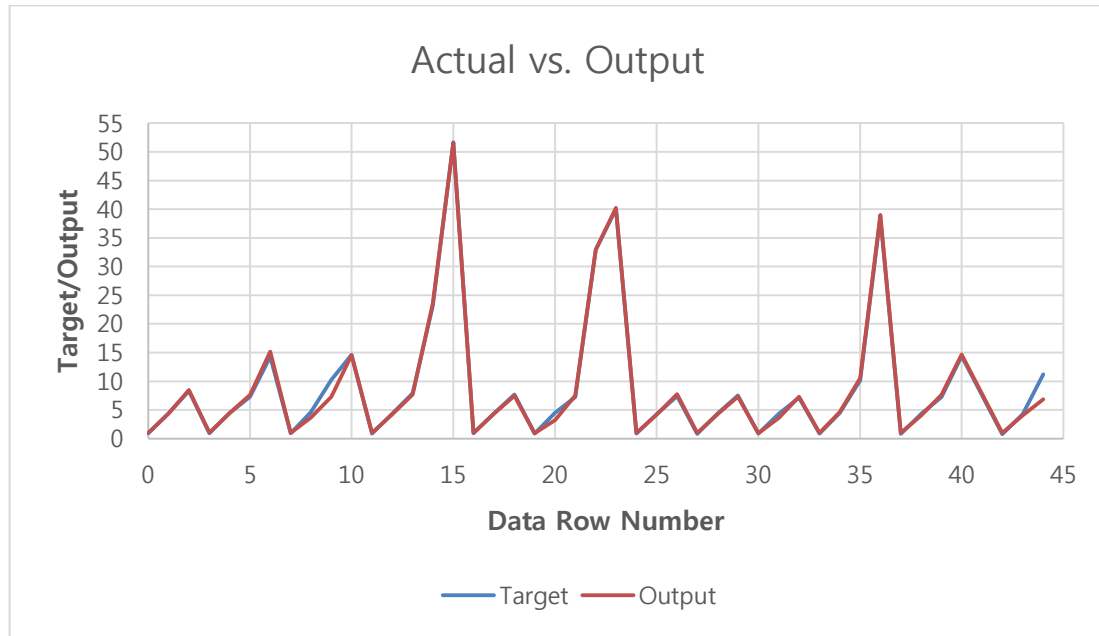


Fig. 7 Comparison of actual values and estimated output values for Model-II infill wall

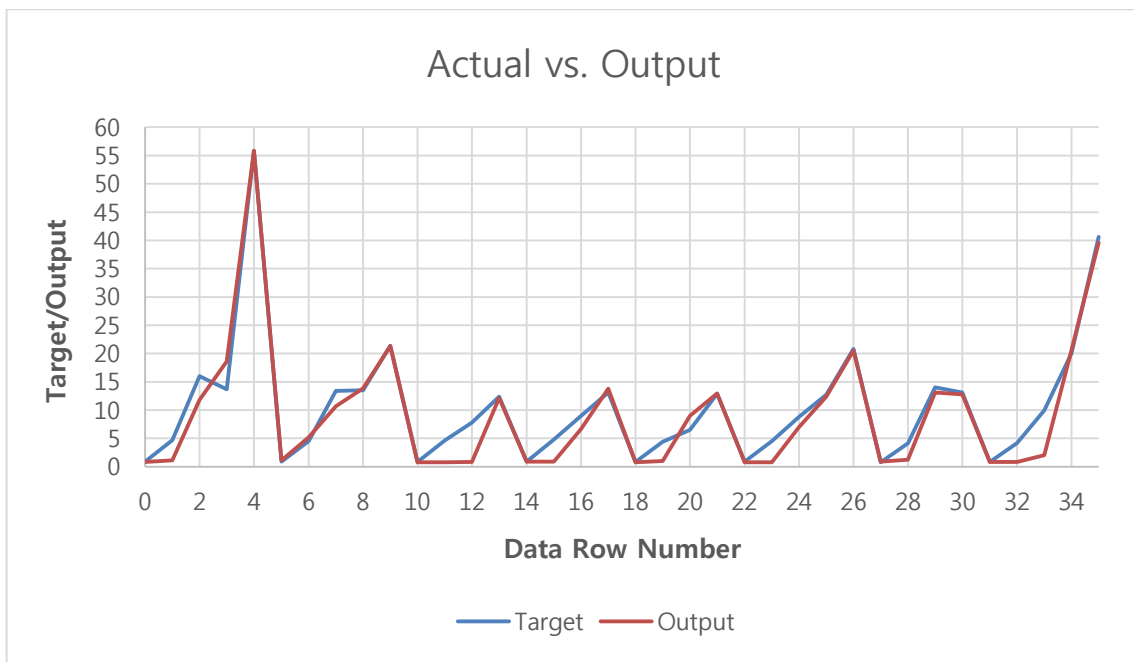


Fig. 8 Comparison of actual values and estimated output values for Model-II RCF

and 6 test data points for the RCF, respectively. Similarly, Model-II has 31 training, 7 validation, and 7 test data points for the infill wall and 24 training, 6 validation, and 6 test data points for the RCF. The automatic architecture search module has an $[x-y-z]$ architecture. This means that the system selects z hidden layers as well as y hidden neurons. x refers to the number of inputs. Because our study consists of two models, we run both models for the infill wall and the RCF. We used an initial learning rate of 0.1 and a momentum of 0.1. We tried alternative values for both the

learning rate and momentums of 0.1 to 2.0 along with various learning algorithms such as Quasi-Newton, Levenberg–Marquardt, Quick Propagation, and Online-Back Propagation. A total of 400 various models were tried. The best networks and their parameters for four ANN models are given in Table 6.

The plots related to the comparison of actual and output values for Model-I and Model-II are acquired respectively as shown in Figs. 5-8. “Data row number” in Figs. 5-8 refers to the sequence number of the total data used. The

Table 7 ANN predicted response of infill wall and RCF for Model-I in terms of absolute maximum displacement (mm) at 0.79 g ground motion level

	VA1	VA2	VA3	VA4
HA5	15.16	16.84	14.79	15.55
HA4	12.64	15.96	13.95	13.81
HA3	16.22	16.20	16.20	15.43
HA2	15.34	15.60	15.60	15.94
HA1	13.80	18.03	18.03	13.80

Table 8. Comparison of experimental and ANN predicted infill wall response in terms of absolute maximum displacement of BJR model at 0.59 g ground motion level

	VA1		VA2		VA3		VA4	
	Experimental (mm)	ANN Predicted (mm)						
HA5	13.7	---	13.1	---	20	---	12.4	---
HA4	38.6	38.16	*	21.93	23.2	23.3	*	36.41
HA3	14.4	14.65	*	11.66	*	12.32	14.3	15.16
HA2	*	10.4	*	31.12	33	32.92	14.6	14.58
HA1	13.5	---	12.9	---	12.7	---	13.1	---

* Sign refers missing data, --- Sign refers omitted data for ANN prediction at 0.59 g PGA level experimental step

Table 9 Comparison of experimental and ANN predicted infill wall and RCF response in terms of absolute maximum displacement of BJR model at 0.74g ground motion level

	VA1		VA2		VA3		VA4	
	Experimental (mm)	ANN Predicted (mm)						
HA5	55.82	55.82	*	19.02	40.6	39.57	*	55.62
HA4	*	51.57	*	51.52	51.7	51.53	*	51.6
HA3	73.9	50.03	*	49.96	*	50.26	*	50.76
HA2	*	40.61	*	39.71	40.0	40.25	*	42.8
HA1	21.4	21.3	*	20.73	20.8	20.51	*	25.95

* Sign refers missing data

total data consist of training, test, and validation data. Separate plots for training, test, and validation data of each model have not been provided because the results given in

Figs. 5-8 are given to evaluate the performance of ANN models prior to missing data prediction and to make further predictions about what would happen in a run with 0.79 g PGA, in other words, to extrapolate predictions.

The horizontal axis represents the data row number (including training, validation, and test data sets), and the vertical axis represents the target and output values. The greater the overlapping points in this graph, the higher the accuracy of the designed ANN model. A comparison between our results and field data shows satisfactory accuracy of the models for the absolute maximum out-of-plane displacement. After verifying the accuracy of the ANN models, missing data are predicted for Model-I and Model-II. For Model-I, missing data are not observed until the end of the

experiment. Due to heavy cracks and the brittle behavior of the unreinforced infill wall, the shake table experiment is terminated at the end of the 0.53 g PGA level. The reason for terminating this experiment at the 0.53 g PGA level is to prevent further damage to the test setup. Therefore, the failure mode and failure level of the PGA are unknown. To predict further behavior and the earthquake resistance level of the unreinforced brick infill wall, missing data are predicted as shown in Table 7.

The shake table experiment is conducted until the end of the 0.74 g PGA level for Model-II. Model-II comprises a reinforced brick infill wall with BJR. During the test series on Model-II, missing data observed at the 0.59 g PGA level due to partial collapse of plaster on the wall are presented in Table 8. In Table 8, it can be observed that the RCF contribution to the missing data is nil. For this reason, ANN prediction is not performed for the RCF at the 0.59 g PGA

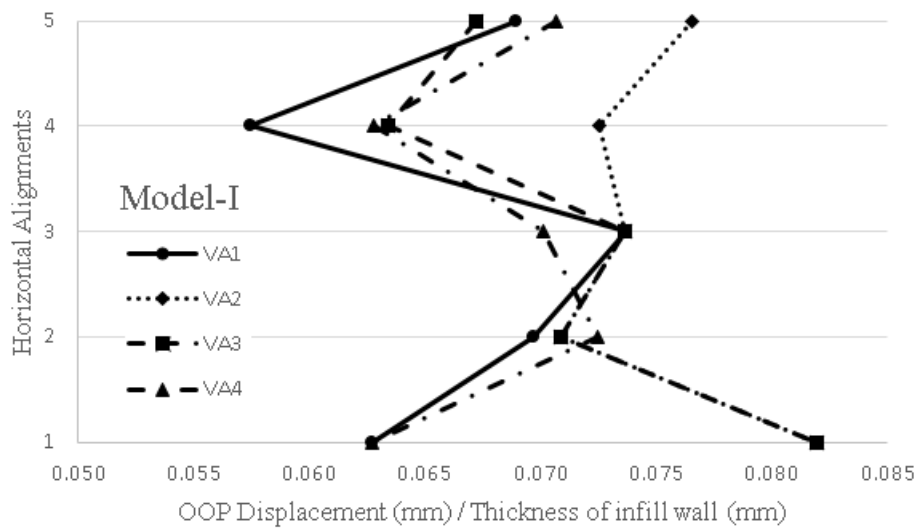


Fig. 9 Profiles of absolute maximum out-of-plane displacement for Model-I at 0.79g PGA level

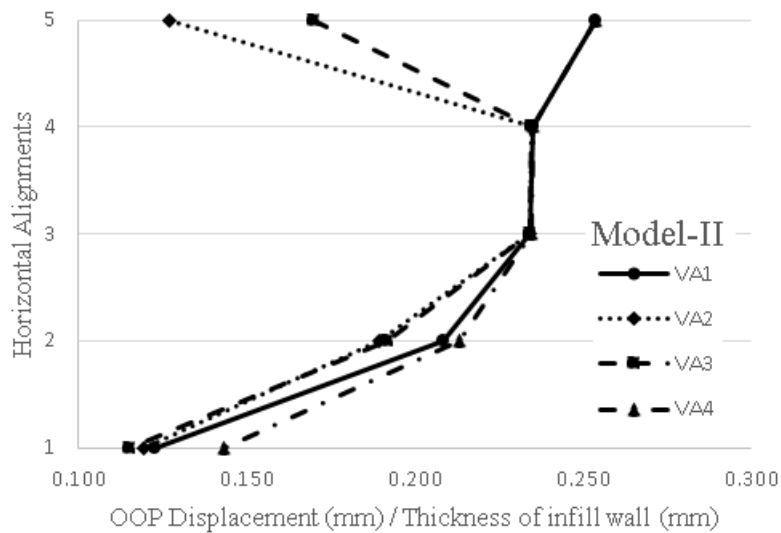


Fig. 10 Profiles of absolute maximum out-of-plane displacement for Model-II at 0.79 g PGA level

level. A comparison of experimental and predicted data is presented in Table 8 at the 0.59 g PGA level. In Table 8, missing data are denoted by the (*) sign and unpredicted data are denoted by the (---) sign. There is no need to construct a prediction model for available data belonging to the RCF for Model-II.

After the 0.59 g PGA level, the last step shake table experiment is carried out on the Model-II test specimen. The PGA level of the last step for Model-II is 0.74 g. During this last step, many heavy cracks occurred, and a large part of the infill wall partially collapsed. Most of the data were missed, because before starting the test, accelerometers were removed from the wall to prevent damage to them. However, after partial collapse of the infill wall and the occurrence of heavy cracks, data were missed as seen in Table 9.

After constructing the ANN model for Model-II, the response of the infill wall and the RCF is predicted for the 0.79 g PGA level (Table 10). A PGA level of 0.79 g is the selected collapse limit of the infill wall determined by the PGA levels of destructive earthquakes. This PGA level is necessary to compare the predicted absolute maximum out-of-plane displacement of both models. The purpose of the comparison is to clearly demonstrate the contribution of BJR as a reinforcing technique for the infill wall.

The expected behavior of the infill wall after reinforcement with BJR includes a large improvement in ductility. After predicting data at the 0.79 g PGA level for both models, their behavior is presented in Figs. 9 and 10.

During the earthquake, due to in-plane forces, the infill wall is damaged step by step while dissipating the earthquake load in the in-plane direction.

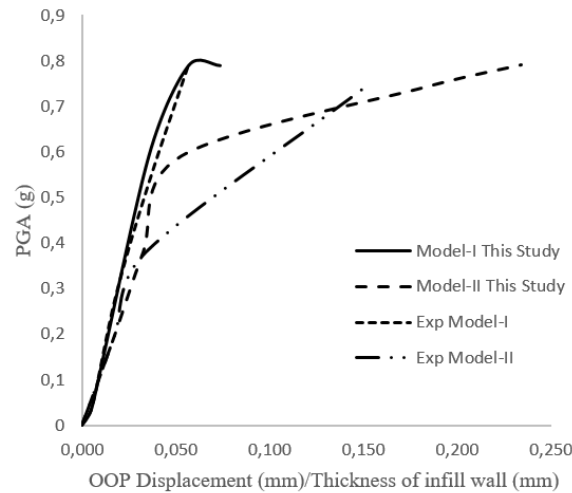


Fig. 11 Comparison of experimental OOP displacement ratio of infill wall and OOP displacement prediction of ANN

Table 10 ANN predicted response of infill wall and RCF for Model-II in terms of absolute maximum displacement at 0.79 g ground motion

	VA1	VA2	VA3	VA4
HA5	55.82	27.91	37.39	55.77
HA4	51.67	51.66	51.66	51.68
HA3	51.53	51.48	51.50	51.60
HA2	45.90	41.67	42.15	46.91
HA1	26.98	26.24	25.39	31.55

However, after increasing inertial forces in the out-of-plane direction, an unexpected failure occurred. BJR contributes to ductility as seen in Fig. 10, unlike URB in Fig. 10. Fig. 9 is plotted to show the failure mode of the infill wall under strong shaking. The Figs. 9 and 10 show the out-of-plane displacements of both models predicted at the same PGA level, that is, 0.79 g, to compare qualitatively the performance of the used reinforcement technique. This prediction is necessary due to the unexpected difference between the target and the achieved PGA level of both shake table experiment models, which are URB and BJR. The forecasting ANN model demonstrated the obviously ductility of the BJR model in comparison with URB. Onat (2015) reported that the BJR model exhibits more ductility than the URB model at the same earthquake excitation. For this reason, the URB model is more prone to collapse with small out-of-plane displacements. Figs. 9 and 10 supported the reported study with an ANN forecasting model.

Fig. 11 is the demonstration and comparison of geometrically nonlinearity of the tested two specimens and ANN prediction of two models. Meanwhile plotting capacity curve, OOP displacements are obtained from center part of the infill and masonry walls commonly. In this study, due to removing instrumentation on the wall, center OOP displacement could not have measured with any device, mid-displacements were plotted only with displacements obtained from accelerometer # 2 located on

the intersection point of HA2 and VA3. Whereas, with a robust prediction of missing value of accelerometer # 6 and accelerometer # 7 real seismic behavior was plotted in Fig. 11. ANN predicted capacity graph of Model-I shows similar OOP behavior in the literature especially with Lagomarsino's study (2015). However, behavior of Model-II is a new behavior due to Bed Joint Reinforcement technique.

5.2 Results of MLR models

Regression analysis is a statistical method capable of handling a wide variety of data patterns (Gul and Guneri 2016a). In MLR models, a variable of interest is identified and treated as dependent on other variables that are called independent variables, which hypothetically affect the value of the dependent variable. In this study, a regression model including one dependent variable—the absolute maximum out-of-plane displacement—and four independent variables labeled X_1 , X_2 , X_3 , and X_4 representing the PGA, local weight, vertical distance from STRUT, and horizontal distance from STRUT is presented. The general form of this model is as follows

$$\text{Predicted } |\text{maximum out of plane displacement}| = \beta_0 + \beta_1 X_1 + \beta_2 X_2 + \beta_3 X_3 + \beta_4 X_4 \quad (6)$$

In this equation, β_0 is the expected intercept, and β_1 is the expected impact on the predicted absolute maximum out-of-plane displacement when X_1 is changed by one unit and is interpreted similar to β_2 , β_3 , and β_4 . In this study, the Minitab 17 statistical tool is used to generate MLR models. The predicted MLR models and the values related to them are displayed in Table 10. According to the results of the MLR models, whereas PGA is statistically significant at the 5% confidence interval, the other three variables have no statistical significance at the same confidence level. Only the β_3 variable shows a different result with a p-value of 0.003. URB with RCF is the model with the highest accuracy (93.2% R^2 and 1.30429 average error) among the models.

Table 10 Results of MLR models

	Model-I (URB)		Model-II (BJR)	
	Infill wall	RCF	Infill wall	RCF
Coefficients and p -values for predictors				
<i>Constant</i> (β_0)	1.599 (0.198)*	-3,129 (0.356)	-1.333 (0.853)	7.76 (0.634)
<i>PGA</i> (β_1)	23.813 (0.000)	24.301 (0.000)	54.521 (0.000)	35.906 (0.000)
<i>local weight</i> (β_2)	0.670 (0.882)	4.613 (0.341)	6.56 (0.806)	-7.72 (0.742)
<i>vertical distance from strut</i> (β_3)	-0.6131 (0.223)	0.5279 (0.003)	-1.197 (0.698)	-1.4018 (0.091)
<i>horizontal distance from strut</i> (β_4)	0.0453 (0.687)	-0.1132 (0.293)	-0.8894 (0.202)	-0.6425 (0.226)
Average Error	1.48023	1.30429	8.82556	6.74195
R^2	90.3%	93.2%	68.0%	68.2%
R^2 (adjusted)	89.4%	92.2%	64.8%	64.1%
p -value for regression (ANOVA)	0.000	0.000	0.000	0.000

*Bolds given in brackets represent p -values, $p < 0.05$ shows significance statistically

Table 11 Comparison of the prediction methods in terms of R^2 and error values

Model criterion	evaluation	Prediction method	Model-I (URB)		Model-II (BJR)	
			Infill wall	RCF	Infill wall	RCF
Average error		ANN	0.9977	0.7099	0.2590	3.6180
		MLR	1.4802	1.3043	8.8256	6.7419
R^2		ANN	98.61%	99.24%	99.97%	96.62%
		MLR	90.30%	93.20%	68.00%	68.20%

5.3 Comparison and discussion

Following the evaluations of the ANN and MLR models, a comparison is carried out in order to identify which methods and models better represent the variability. A comparison of the results of these two methods in terms of predicting the absolute maximum out-of-plane displacement shows that ANN-based models have higher R^2 values and lower values of average error than the MLR models (as shown in Table 11).

6. Conclusions

Civil engineering applications may need an experimental test setup with expensive instruments. During these experiments, recording data sometimes cannot be gathered due to damage to instruments, or the recording process may be deliberately terminated to prevent damage to the instruments. Experimental evaluation of the out-of-plane response of the infill wall under an earthquake load is difficult due to the slenderness of the infill wall in the out-of-plane direction. The experimental test may suffer from missing data due to early removal of the recording instruments.

In this study, an ANN-based prediction model is proposed for the absolute maximum out-of-plane displacement of the infill wall. To this end, two shake table experiments are

selected as URB and BJR. Initially, four ANN models (URB and BJR models for each of the infill wall and the RCF) are constructed to demonstrate the accuracy performance. A comprehensive analysis is then conducted for missing data prediction and for making further predictions about what would happen in a run with 0.79 g PGA; in other words, extrapolating predictions are performed. A high level of accuracy was obtained in the prediction of missing data. In addition, absolute maximum displacements were predicted accurately for both models at the 0.79 g PGA level to plot the out-of-plane failure mode of the infill wall at the time of its total collapse. The proposed models take the PGA, local weight, vertical distance from STRUT, and horizontal distance from STRUT as the predictors. In order to validate the prediction models and make an original contribution to the literature, a comparison with MLR is also provided. The results of the comparison show that ANN-based models provide better results than regression-based models in terms of the average error and R^2 .

To sum up, this study is aimed at (1) predicting the missing absolute maximum out-of-plane displacement response of the infill wall and RCF as an appropriate subject of civil engineering, (2) showing which prediction methods and models better measure the variability on the basis of two important statistical parameters: R^2 and the average error, and (3) assisting stakeholders by decreasing the cost of shake table experiments with the aid of data

prediction after the removal of devices from the tested specimen.

Some limitations in this study should be acknowledged. The first limitation concerns the predictors (independent variables of the ANN model). The analyzed independent variables in this study depend solely on four parameters. The second potential limitation is that the analysis of the current study is mainly for ANN and MLR solutions. A possible extension of the study is an investigation of the same problem with other methods such as adaptive-network-based fuzzy inference systems and/or support vector machine, which is left for future works. In addition, more work can be performed on the out-of-plane failure mechanisms of masonry walls. Application of ANNs to the prediction of the out-of-plane response of masonry walls subjected to shake table excitation can be carried out. To apply this model any of shake table experiment, it should be drawn attention some points as below;

- Prior to the prediction, there should be minimum three experiments with un-missing data.
- While minimum two of the four experiment data should be in the linear phase, minimum two experimental data should be available in non-linear phase of experiment.
- Nonlinear functions should be used in missing data prediction and as well as in make further predictions about what would happen in a run with 0.79 g PGA.
- The data set chosen in this study has some particular characteristics such as location of accelerometers (vertical and horizontal distance from strut) and differential weight that effects each accelerometer.

References

- Al-Chaar, G., Issa, M. and Sweeney, S. (2002), "Behaviour of masonry-infilled nonductile reinforced concrete frames", *J. Struct. Eng. -ASCE*, **128**(8), 1055-1063.
- Alyuda (2017), Neural networks software, Alyuda Research LLC, Cupertino CA. Available from <http://www.al-yuda.com/neural-networks-software.htm>
- Anil, Ö. and Altın, S. (2007), "An experimental study on reinforced concrete partially infilled frames", *Eng. Struct.*, **29**, 449-460.
- Bilgehan, M., Gürel, M.A., Pekgökgöz, R.K. and Kısa, M. (2012), "Buckling load estimation of cracked columns using artificial neural network modeling technique", *J. Civil Eng. Manage.*, **18**(4), 568-579.
- Calvi, G. and Bolognini, D. (2001), "Seismic response of reinforced concrete frames infilled with weakly reinforced masonry panels", *J. Earthq. Eng.*, **5**(2), 153-185.
- Correia, A.A., Costa, A.C., Candeias, P. and Lourenço, P.B. (2014), "Ensaio sísmico inovadores de pórticos com paredes de enchimento em alvenaria", 5as Jornadas Portuguesas de Engenharia de Estruturas (JPEE 2014), 1-16.
- D'Ayala, D. and Shi, Y. (2011), "Modeling masonry historic buildings by multi-body dynamics", *Int. J. Architect. Heritage*, **5**(4-5), 483-512.
- Dolšek, M. and Fajfar, P. (2002), "Mathematical modelling of an infilled RC frame structure based on the results of pseudo-dynamic tests", *Earthq. Eng. Struct. D.*, **31**(6), 1215-1230.
- Efendigil, T., Ö nüt, S. and Kahraman, C. (2009), "A decision support system for demand forecasting with artificial neural networks and neuro-fuzzy models: A comparative analysis", *Exp. Syst. Appl.*, **36**(3), 6697-6707.
- Facchini, L., Betti, M. and Biagini, P. (2014), "Neural network based modal identification of structural systems through output-only measurement", *Comput. Struct.*, **138**, 183-194.
- Fahmy, A.S., El-Madawy, M.E.T. and Gobran, Y.A. (2016), "Using artificial neural networks in the design of orthotropic bridge decks", *Alexandria Eng. J.*, **55**(4), 3195-3203.
- Furtado, A., Rodrigues, H., Arêde, A. and Varum, H. (2016), "Experimental evaluation of out-of-plane capacity of masonry infill walls", *Eng. Struct.*, **111**, 48-63.
- Garzón-Roca, J., Adam, J.M., Sandoval, C. and Roca, P. (2013), "Estimation of the axial behaviour of masonry walls based on artificial neural networks", *Comput. Struct.*, **125**, 145-152.
- Graziotti, F., Tomassetti, U., Penna, A. and Magenes, G. (2016), "Out-of-plane shaking table tests on URM single leaf and cavity walls", *Eng. Struct.*, **125**, 455-470.
- Gul, M. and Guneri, A.F. (2015), "Forecasting patient length of stay in an emergency department by artificial neural networks", *J. Aeronaut. Sp. Technol. (Havacılık ve Uzay Teknolojileri Dergisi)*, **2**(8), 1-6.
- Gul, M. and Guneri, A.F. (2016), "An artificial neural network-based earthquake casualty estimation model for Istanbul city", *Nat. Hazards*, **84**(3), 2163-2178.
- Gul, M. and Guneri, A.F. (2016a), "Planning the future of emergency departments: Forecasting ED patient arrivals by using regression and neural network models", *Int. J. Ind. Eng.: Theory, Appl. Pract.*, **23**(2), 137-154.
- Guneri, A.F. and Gumus, A.T. (2008), "The usage of artificial neural networks for finite capacity planning", *Int. J. Ind. Eng.: Theory, Appl. Pract.*, **15**(1), 16-25.
- Guneri, A.F. and Gumus, A.T. (2009), "Artificial neural networks for finite capacity scheduling: a comparative study", *Int. J. Ind. Eng.: Theory, Appl. Pract.*, **15**(4), 349-359.
- Hakim, S.J.S. and Razak, H.A. (2014), "Modal parameters based structural damage detection using artificial neural networks-a review". *Smart Struct. Syst.*, **14**(2), 159-189.
- Hasançebi, O. and Dumlupınar, T. (2013), "Linear and nonlinear model updating of reinforced concrete T-beam bridges using artificial neural networks", *Comput. Struct.*, **119**, 1-11.
- Hashemi, A. and Mosalam, K.M. (2006), "Shake-table experiment on reinforced concrete structure containing masonry infill wall", *Earthq. Eng. Struct. D.*, **35**(14), 1827-1852.
- Hoła, J. and Schabowicz, K. (2005), "Application of artificial neural networks to determine concrete compressive strength based on non-destructive tests", *J. Civil Eng. Manage.*, **11**(1), 23-32.
- Joshi, S.G., Londhe, S.N. and Kwatra, N. (2014), "Application of artificial neural networks for dynamic analysis of building frames", *Comput. Concrete*, **13**(6), 765-780.
- Kisi, O. and Kerem Cigizoglu, H. (2007), "Comparison of different ANN techniques in river flow prediction", *Civil Eng. Environ. Syst.*, **24**(3), 211-231.
- Kröse, B., Krose, B., van der Smagt, P. and Smagt, P. (1993), "An introduction to neural networks", *CRC Press*, London.
- Kumar, B. and Samui, P. (2008), "Application of ANN for predicting pore water pressure response in a shake table test", *Int. J. Geotech. Eng.*, **2**(2), 153-160.
- Lagomarsino, S. (2015), "Seismic assessment of rocking masonry structures", *Bull. Earthq. Eng.*, **13**(1), 97-128.
- Lee, S.C. and Han, S.W. (2002), "Neural-network-based models for generating artificial earthquakes and response spectra", *Comput. Struct.*, **80**(20), 1627-1638.

- Lourenço, P.B., Leite, J.M., Paulo Pereira, M.F., Campos-Costa, A., Candeias, P.X. and Mendes, N. (2016), "Shaking table testing for masonry infill walls: unreinforced versus reinforced solutions", *Earthq. Eng. Struct. D.*, **45**(14), 2241-2260.
- Mendes, N. (2012), "Seismic assessment of ancient masonry buildings: shaking table tests and numerical analysis", PhD Thesis, University of Minho, Guimaraes, Portugal.
- Misir, I.S., Ozcelik, O. and Kahraman, S. (2015), "The Behaviour of double-whyte hollow clay brick walls under bidirectional loads in R/C frame", *Teknik Dergi*, **26**(3), 7139-7165.
- Misir, I.S., Ozcelik, O., Girgin, S.C. and Yucel, U. (2016), "The behavior of infill walls in RC frames under combined bidirectional loading", *J. Earthq. Eng.*, **20**(4), 559-586.
- Misir, S., Ozcelik, O., Girgin, S.C. and Kahraman, S. (2012), "Experimental work on seismic behavior of various types of masonry infilled RC frames", *Struct. Eng. Mech.*, **44**(6), 763-774.
- Mosalam, K. and Günay, M.S. (2015), "Progressive collapse analysis of RC frames with URM infill walls considering inplane/out-of-plane interaction", *Earthq. Spectra*, **31**(2), 921-943.
- Onat, O. (2015), "Investigation of seismic behaviour of infill wall surrounded by reinforced concrete frame", Joint PhD Thesis, Yıldız Technical University Istanbul Turkey & Minho University, Guimaraes Portugal.
- Onat, O., Lourenco, P.B. and Kocak, A. (2015), "Experimental and numerical analysis of RC structure with two leaf cavity wall subjected to shake table", *Struct. Eng. Mech.*, **55**(5), 1037-1053.
- Onat, O., Lourenco, P.B. and Kocak, A. (2016), "Nonlinear analysis of RC structure with massive infill wall exposed to shake table", *Earthq. Struct.*, **10**(4), 811-828.
- Pereira, M.F.P. (2013), Avaliação do desempenho das envolventes dos edifícios face à acção dos sismos (in Portuguese). Department of Civil Engineering, University of Minho. PhD.
- Pujol, S. and Fick, D. (2010), "The test of a full-scale three-story RC structure with masonry infill walls", *Eng. Struct.*, **32**(10), 3112-3121.
- Rizzo, P. and Lanza, D.S. (2006), "Wavelet-based feature extraction for automatic defect classification in strands by ultrasonic structural monitoring", *Smart Struct. Syst.*, **2**(3), 253-274.
- Sakla, S.S. and Ashour, A.F. (2005), "Prediction of tensile capacity of single adhesive anchors using neural networks", *Comput. Struct.*, **83**(21), 1792-1803.
- Shan, S., Li, S., Xu, S. and Xie, L. (2016), "Experimental study on the progressive collapse performance of RC frames with infill walls", *Eng. Struct.*, **111**, 80-92.
- Shawa, O.A., Felice, G., Mauro, A. and Sorrentino, L. (2012), "Out-of-plane seismic behaviour of rocking masonry walls", *Earthq. Eng. Struct. D.*, **41**(5), 949-968.
- Shi, Y.N. (2016), "Dynamic behaviour of masonry structures", PhD dissertation, University of Bath, UK.
- Shing, P.B. and Mehrabi, A.B. (2002), "Behaviour and analysis of masonry-infilled frames", *Prog. Struct. Eng. Mater.*, **4**(3), 320-331.
- Šipoš, T.K., Sigmund, V. and Hadzima-Nyarko, M. (2013), "Earthquake performance of infilled frames using neural networks and experimental database", *Eng. Struct.*, **51**, 113-127.
- Somoza, E. and Somoza, J.R. (1993), "A neural-network approach to predicting admission decisions in a psychiatric emergency room", *Medical Decis. Making*, **13**(4), 273-280.
- Stavridis, A., Koutromanos, I. and Shing, P.B. (2012), "Shake-table tests of a three-storey reinforced concrete frame with masonry infill walls", *Earthq. Eng. Struct. D.*, **41**, 1089-1108.
- Topçu, İ.B., Boğa, A.R. and Hocaoglu, F.O. (2009), "Modeling corrosion currents of reinforced concrete using ANN", *Autom. Constr.*, **18**(2), 145-152.
- Tu, Y.H., Chuang, T.H., Liu, P.M. and Yang, Y.S. (2010), "Out-of-plane shaking table tests on unreinforced masonry panels in RC frames", *Eng. Struct.*, **32**(12), 3925-3935.
- Vaculik, J., and Griffith, M.C. (2017), "Out-of-plane shaketable testing of unreinforced masonry walls in two-way bending", *Bull. Earthq. Eng.*, 1-38.
- Varela-Rivera, J.L., Navarrete-Macias, D., Fernandez-Baqueiro, L., E. and Moreno, E.I. (2011), "Out-of-plane behaviour of confined masonry walls", *Eng. Struct.*, **33**, 1734-1741.
- Varela-Rivera, J., Polanco-May, M., Fernandez-Baqueiro, L. and Moreno, E.I. (2012), "Confined masonry walls subjected to combined axial loads and out-of-plane uniform pressures", *Can. J. Civil Eng.*, **39**, 439-447.
- Yön, B., Sayın, E. and Onat, O. (2017), Earthquakes and Structural Damages. In Earthquakes-Tectonics, Hazard and Risk Mitigation. InTech book edited by Taher Zouaghi, ISBN 978-953-51-2886-1, Print ISBN 978-953-51-2885-4; DOI: 10.5772/65425.

CC